

Electromagnetic properties of the low-lying states in heavy ($A \simeq 190$) transitional nuclei

C. Baktash

*Physics Department, Brookhaven National Laboratory, Upton, New York 11973**
and Physics Department, University of Pittsburgh, Pittsburgh, Pennsylvania 15260

J. X. Saladin, J. J. O'Brien,[†] and J. G. Alessi[‡]

Physics Department, University of Pittsburgh, Pittsburgh, Pennsylvania 15260

(Received 30 July 1980)

In a particle- γ spectroscopy experiment, $^{188,190,192}\text{Os}$ nuclei were Coulomb excited by 14.5 MeV ^4He , 48.0 MeV ^{16}O , and 62.0 MeV ^{32}S beams, successively. Using both semiclassical and quantum mechanical coupled channels codes, the coincidence γ -ray yields were analyzed to obtain the relative quadrupole moments of the 2_1^+ state, as well as branching ratios and the spectroscopic quadrupole moments of the 2_2^+ states in these nuclei. As an independent check, the spectroscopic quadrupole moments of the 2_1^+ and 2_2^+ states in ^{188}Os were measured by particle spectroscopy techniques using ^{16}O projectiles. The results of the two experiments are in good agreement. These results, together with the corresponding values for $^{184,186}\text{W}$ and ^{194}Pt , are compared with the predictions of several models, including (i) microscopic pairing-plus-quadrupole and boson expansion theory, and (ii) phenomenological interacting boson approximation and asymmetric rigid rotor models. The general experimental trends are best described by the above microscopic models. Both phenomenological models fail to reproduce the systematics of the experimental quadrupole moments.

NUCLEAR REACTIONS $^{188,190,192}\text{Os}(\alpha, \alpha'\gamma)$, $E = 14.5$ MeV; $^{188,190,192}\text{Os}(^{16}\text{O}, ^{16}\text{O}'\gamma)$, $E = 48.0$ MeV; $^{188,190,192}\text{Os}(^{32}\text{S}, ^{32}\text{S}'\gamma)$, $E = 62.0$ MeV; measured particle- γ coin; deduced $q(2_2^+)$, branching ratios (2_2^+), relative $q(2_1^+)$. Thick natural target. $^{188}\text{Os}(^{16}\text{O}, ^{16}\text{O}'\gamma)$, $E = 45.0$ MeV; measured $\sigma(E, 142.3^\circ)$; deduced $q(2_1^+)$, $q(2_2^+)$. Thin enriched target. Coupled channel semiclassical and quantum mechanical analyses.

I. INTRODUCTION

The Os-Pt nuclei, spanning a region where a prolate to oblate shape transition takes place, provide a crucial testing ground for the nuclear structure models that attempt to describe the collective degrees of freedom. The spectroscopic quadrupole moments¹⁻³ $q(2_1^+)$ as well as the systematics of the relative location of the quasigamma band with respect to the ground state band, suggest that the γ degree of freedom plays an important role in this shape transition region. While all models agree that these nuclei are to varying degrees triaxial, they differ on the nature of this triaxiality.

In the pairing plus quadrupole model of Kumar and Baranger,⁴ the potential energy surfaces (PES) are predicted to be soft with respect to γ vibrations in the $A \simeq 190$ mass region. The predicted PES are similar to those obtained from other semimicroscopic calculations in this region,⁵⁻⁸ which attribute the triaxiality to dynamics, that is, zero-point fluctuations. The same conclusion has been reached in some phenomenological models,^{9, 10} as well as in a Hartree-Fock-Bogoliubov microscopic calculation¹¹ which has found appreciable *dynamic* triaxiality for most nuclei investigated.

In contrast, some investigators have found that the asymmetric rotor model (ARM) of Davydov and Filippov¹² fits certain features of the transitional nuclei successfully. The rigid triaxial shapes assumed in this model stand at variance with practically all microscopic calculations.

More recently, the interacting boson approximation (IBA) model of Arima and Iachello¹³ has offered an alternative description of the transitional nuclei compared to the above geometrical models which attempt to approximately solve Bohr's collective Hamiltonian. Many of the complex and rapidly changing empirical features of the Os-Pt region are well reproduced in terms of a perturbed O(6) scheme.¹⁴ Since the γ -unstable model of Wilets and Jeans¹⁵ is the closest geometrical analog of the O(6) limit of the IBA,^{14, 16} the success of this model in reproducing the experimental data may be interpreted as additional support for the γ -soft cores in this region.

In view of the fact that nearly all the microscopic calculations predict γ -soft potential energy surfaces, it is important to experimentally determine the extent of the softness of these nuclei with respect to γ vibrations. The rigidity or softness of the PES affects such observables as the energy levels, electromagnetic transition rates, and spectroscopic factors. However, some

of these observables are equally affected by variations in other nuclear parameters and, hence, are not unique tests of the core softness. One exception is the electromagnetic properties of the quasigamma band.¹⁷ This report is part of a systematic study of the electromagnetic properties of the quasigamma band in some even-even W,¹⁸ Os, and Pt (Ref. 17) nuclei. Presented here are the results of Coulomb excitation experiments in which the spectroscopic quadrupole moments and branching ratios of the 2_2^+ states in ^{188,190,192}Os were determined. Although the static quadrupole moments are not very sensitive to the core softness, they enter the determination of the transition matrix elements of the quasigamma band from heavy ion Coulomb excitation experiments. Some of these results have been reported in earlier communications.¹⁹

II. DATA ACQUISITION AND REDUCTION

The experiment consists of consecutively Coulomb exciting a thick, natural Os target by 14.5 MeV ⁴He, 48.0 MeV ¹⁶O, and 62.0 MeV ³²S beams obtained from the University of Pittsburgh 3-stage Van de Graaff. A Ge(Li) detector at 55° was used to detect the deexcitation γ rays in coincidence with backscattered particles which were detected in a cooled surface barrier annular detector at $\langle\theta\rangle_{\text{lab}} = 163^\circ$. To minimize the sensitivity to such factors as target self-absorption and Ge(Li) finite solid angle correction, the target assembly and detection geometry were untouched for the duration of the experiment. The γ -ray energy, particle energy, as well as the timing information were recorded, event by event, on magnetic tape. The data were subsequently analyzed off line, by placing appropriate windows on the particle-energy and timing spectra, and projecting out the corresponding γ -ray spectra. The ratios of the true peak to the accidental background in the timing spectra were better than 20 for the ⁴He and 70 for ¹⁶O and ³²S beams, respectively. Nevertheless, the γ -ray spectra were corrected for the random coincidence events. Details of the experimental setup as well as data reduction procedure are given in Refs. 17 and 18. Sample spectra are given in Figs. 1 to 3.

As an independent check on the $q(2_2^+)$ values obtained from the above particle- γ coincidence experiment, the quadrupole moment of the 2_2^+ state in ¹⁸⁸Os was additionally measured by particle spectroscopy techniques. In this experiment, thin (10–15 $\mu\text{g}/\text{cm}^2$), isotopically enriched (94.47%) spot targets of ¹⁸⁸Os were bombarded with a 45 MeV ¹⁶O beam. The elastically and inelastically scattered particles were momentum analyzed at a

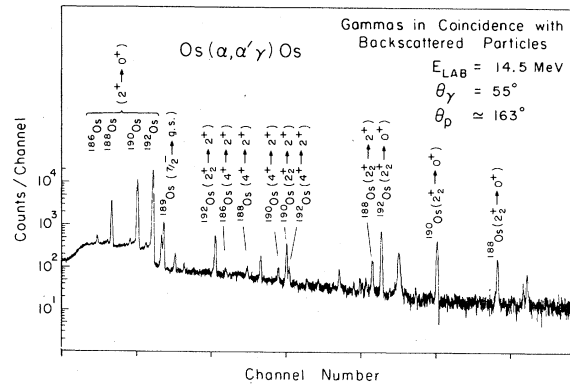


FIG. 1. Particle-gamma coincidence spectrum for 14.5 MeV ⁴He particles.

142.3° laboratory angle in an Enge split-pole magnetic spectrograph. Two position sensitive detectors were placed in the focal plane of the spectrograph to detect the 7⁺ and 8⁺ charge states, which together account for nearly 95% of the outgoing ions. A sample spectrum is shown in Fig. 4.

III. DATA ANALYSIS

The particle data were analyzed to obtain the spectroscopic quadrupole moments of the 2_1^+ and 2_2^+ states in ¹⁸⁸Os. The particle-coincidence data were analyzed to extract the spectroscopic quadrupole moments of the 2_2^+ states in ^{188,190,192}Os isotopes. Also, relative $q(2_1^+)$ values were deduced for ^{190,192}Os nuclei with respect to that of ¹⁸⁸Os. Additionally, this data rendered more precise branching ratios for the 2_2^+ states in all three Os nuclei.

The calculations of the elastic and inelastic scattering cross sections were obtained from the semiclassical coupled channels code of Winther

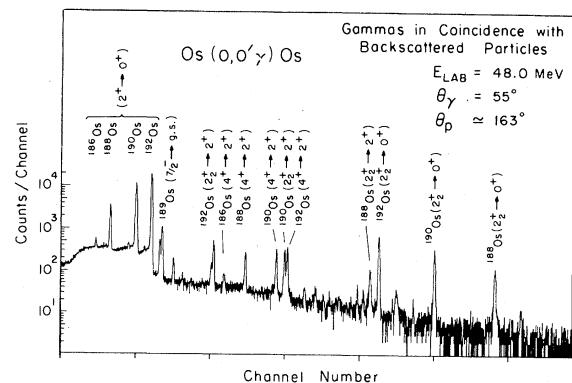


FIG. 2. Particle-gamma coincidence spectrum for 48.0 MeV ¹⁶O particles.

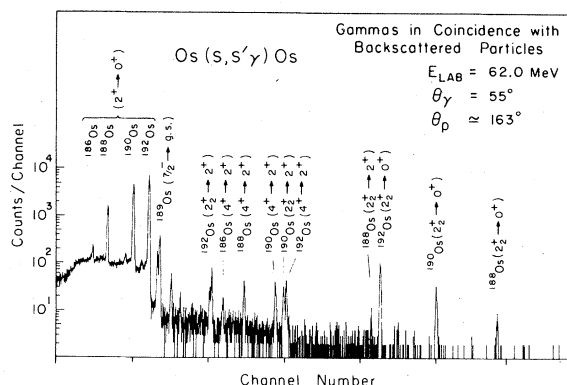


FIG. 3. Particle-gamma coincidence spectrum for 62.0 MeV ^{32}S particles.

and de Boer²⁰ (WD), and included the 0^+ , 2^+ , 4^+ , 6^+ , 2_2^+ , and 4_2^+ levels. The quantum mechanical (QM) correction factors for the 2_1^+ , 2_2^+ , and 4_1^+ states were obtained from the quantum mechanical coupled channels code AROSA²¹ in a manner discussed in Refs. 17 and 18. In the range of beam energies relevant to this experiment, the QM corrections to the 2_2^+ states amounted to nearly 2–2.5% and 1.5% for the ^4He and ^{16}O projectiles, respectively. The corresponding QM corrections for the 2_1^+ states were less than 0.5%.

The relevant $E2$ reduced matrix elements which enter the calculations were obtained from the re-

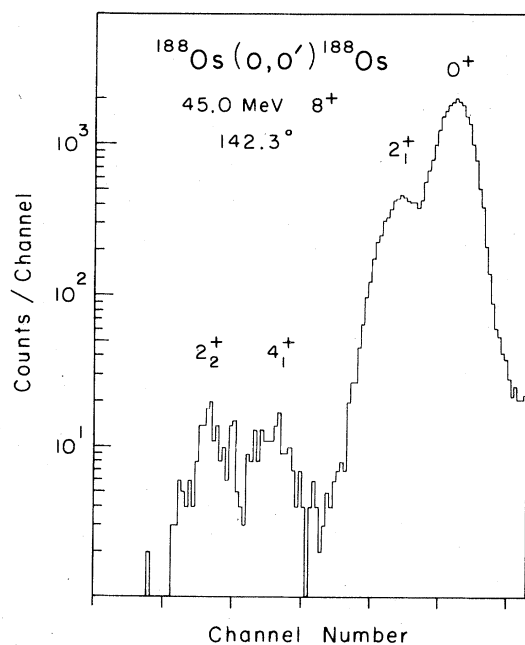


FIG. 4. Spectrum of elastically and inelastically scattered ^{16}O particles.

sults of previous measurements. In cases where more than one measurement was available, the weighted average of the more recent values was adopted. The following studies were consulted in arriving at the choice of the reduced quadrupole matrix elements (M_{E2}): Refs. 1, 2, and 22 for $q(2_1^+)$; Refs. 1, 2, 23, and 24 for $M_{E2}(0^+, 2_1^+)$; Refs. 24 and 25 for $M_{E2}(0^+, 2_2^+)$, $M_{E2}(2_1^+, 2_2^+)$, and $M_{E2}(2_1^+, 4_1^+)$; and Ref. 25 for $M_{E2}(2_2^+, 4_2^+)$, $M_{E2}(4_1^+, 4_2^+)$, and $M_{E2}(4_1^+, 6_1^+)$. Other M_{E2} values were taken from calculations of Kumar and Baranger.⁴ The influence of these M_{E2} on the γ -ray yields from the 2_2^+ states were, however, insignificant. The $M1$ matrix elements were determined from the compilation of the $M1/E2$ mixing ratios by Krane.²⁶ However, it should be pointed out that the effect of $M1$ on the angular distribution of the $2_2^+ \rightarrow 2_1^+$ transition is nearly zero at $\theta = 55^\circ$. Moreover, since the extraction of the quadrupole moments involve comparison of the relative γ -ray yields as a function of beam species, they are independent of the $M1$ values.

The $E4$ transition matrix elements $M_{E4}(0^+, 4_1^+)$ were taken from a Coulomb nuclear interference work by Baker *et al.*²⁷ The rigid rotor model was used to estimate other $E4$ couplings. These $E4$ matrix elements did not exert any discernible influence on the extracted $q(2_2^+)$ values reported in this survey.

In the case of particle- γ data, the thin target γ -ray yields calculated by the WD code had to be integrated over the beam energy and the acceptance angles of the particle and γ -ray detectors. The range of energies included in this integration were ≈ 11.5 – 14.5 MeV for ^4He , 36–48 MeV for ^{16}O , and 46–62 MeV for the ^{32}S projectiles. The values of stopping powers entering the energy integration were taken from the work of Northcliffe and Schilling.²⁸ The finite Ge(Li) solid angle correction factors were based on the extrapolation of values given by Camp and Van Lehn.²⁹ Finally, the thick target yields were evaluated at three scattering angles, and numerically integrated to account for the finite particle-detector solid angle. The thick target yields were corrected for such factors as the target self-absorption and QM effects, which were calculated in a manner described in Ref. 18.

The absolute γ -ray yields from a thick target depend on many factors, including beam intensity, target isotopic enrichment, dead time losses, the effective target thickness and, hence, the stopping power, finite Ge(Li) solid angle correction factors, and the absolute Ge(Li) efficiency. The relative γ -ray yields, however, are either independent, or insensitive to these factors. The extraction of the quadrupole moments were, therefore,

based on yield ratios obtained by normalizing the yields relative to the $(2_1^+ \rightarrow 0^+)$ transition strength. Furthermore, to reduce the sensitivity to many electromagnetic matrix elements which enter the calculation of the yield ratios (Y_R), it was decided to deduce the quadrupole moments by comparing the relative enhancement of the Y_R as a function of beam species. According to the second-order perturbation theory, for a given energy range and under a fixed detection geometry, the dependence of the Y_R on the $q(2_2^+)$ values may be parametrized in terms of the projectile mass A as follows:

$$Y_R(2_2^+ \rightarrow 0^+; A) \equiv \frac{Y(2_2^+ \rightarrow 0^+; A)}{Y(2_1^+ \rightarrow 0^+; A)} \\ = \frac{\epsilon(2_2^+ \rightarrow 0^+)}{\epsilon(2_1^+ \rightarrow 0^+)} \frac{M_{E2}(0^+, 2_2^+)^2}{M_{E2}(0^+, 2_1^+)^2} f(A) \\ \times \frac{1 + \rho_{2_2^+}(A)q(2_2^+) + \alpha(A)\chi(2_2^+)}{1 + \rho_{2_1^+}(A)q(2_1^+)}. \quad (1)$$

Here, $M_{E2}(n, m)$ denotes the reduced quadrupole matrix element connecting states n and m , and $\epsilon(n \rightarrow m)$ indicates the detection efficiency for the $(n \rightarrow m)$ transition γ ray. Functions $\rho_{2_2^+}(A)$, $\rho_{2_1^+}(A)$, and $\alpha(A)$ depend on the experimental conditions and are readily calculable. The parameter $\chi(2_2^+)$ is given by

$$\chi(2_2^+) \equiv M_{E2}(0^+, 2_1^+) \frac{M_{E2}(2_1^+, 2_2^+)}{M_{E2}(2_2^+, 0^+)} \quad (2)$$

and is proportional to the square root of the cascade-to-crossover branching ratio of the 2_2^+ state. While functions $\rho_{2_2^+}(A)$, $\rho_{2_1^+}(A)$, and $\alpha(A)$ depend strongly on the projectile mass, their ratios, namely $\rho_{2_1^+}/\rho_{2_2^+}$ and $\alpha/\rho_{2_2^+}$, are, to a very good approximation, independent of A . Therefore, expansion of Eq. (1) around the experimental values $q_0(2_1^+)$ and $\chi_0(2_2^+)$ results in the expression

$$Y_R(2_2^+ \rightarrow 0^+, A) = g(A) \{ (1 + \rho(A) \{ q(2_2^+) + \beta[q(2_1^+) - q_0(2_1^+)] \\ + \gamma[\chi(2_2^+) - \chi_0(2_2^+)] \}) \}. \quad (3)$$

Again, functions $g(A)$ and $\rho(A)$, as well as parameters β and γ , are fully calculable. Specifically, $g(A)$ may be obtained through a calculation corresponding to

$$q(2_2^+) = 0, \\ q(2_1^+) = q_0(2_1^+),$$

and

$$\chi(2_2^+) = \chi_0(2_2^+).$$

Similarly, $\rho(A)$ may be readily obtained by assuming a nonzero $q(2_2^+)$ in the computation. Consequently, a plot of $[Y_R]_{\text{exp}}/g(A)$ as a function of the sensitivity parameter, $\rho(A)$, will be a linear

function whose slope determines the $q(2_2^+)$:

$$\text{slope} = q(2_2^+) + \beta[q(2_1^+) - q_0(2_1^+)] \\ + \gamma[\chi(2_2^+) - \chi_0(2_2^+)]. \quad (4)$$

The y intercept of this linear plot is proportional to

$$\frac{\epsilon(2_2^+ \rightarrow 0^+)}{\epsilon(2_1^+ \rightarrow 0^+)} \left[\frac{M_{E2}(0^+, 2_2^+)}{M_{E2}(0^+, 2_1^+)} \right]^2$$

and may be different than 1.0 if the actual values differ from those used in the calculation. In this case, the "true slope" will be the ratio of the experimental slope divided by the y intercept. The quadrupole moment is, therefore, given by

$$q(2_2^+) = \text{true slope} - \beta[q(2_1^+) - q_0(2_1^+)] \\ - \gamma[\chi(2_2^+) - \chi_0(2_2^+)]. \quad (5)$$

Figure 5 shows the sensitivity plot for ^{192}Os . Shown on this plot are six points, corresponding to three beams and two yield ratios $Y_R(2_2^+ \rightarrow 0^+)$ and $Y_R(2_2^+ \rightarrow 2_1^+)$. The error bars are due to experimental uncertainties from such sources as the statistical fluctuations, background subtraction, and contaminations due to other transitions in the case of composite peaks. The solid and dashed lines were obtained from a least-squares fit to the experimental points and denote the true slope and the associated uncertainties, respectively. For comparison, the dot-dashed line represents the slope corresponding to $q(2_2^+) = 0.34$ e b, which has been predicted by Kumar and Baranger.⁴

According to Eq. (5), the deduced $q(2_2^+)$ depends on $q(2_1^+)$ as well as the sign and magnitude of

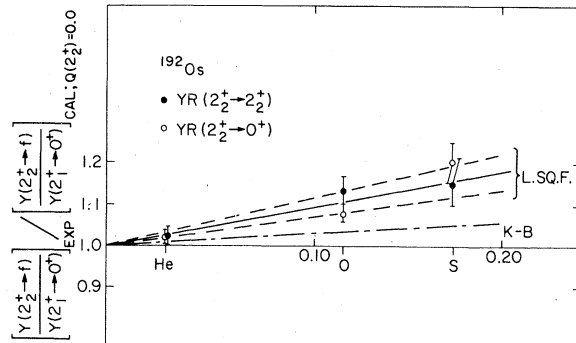


FIG. 5. Plot of the ratios of the experimental and calculated yield ratios $[Y_R(2_2^+ \rightarrow f)]$ as a function of sensitivity parameter $\rho(A)$ (see text). The slope of the fitted line (solid line) is proportional to $q(2_2^+)$. For comparison, the dot-dashed line represents the slope corresponding to $q(2_2^+) = 0.34$ e b which is predicted by Kumar and Baranger (Ref. 4).

$\chi(2_2^+)$. The experimental $q_0(2_1^+)$ values used in the calculation were based on the weighted average of the quadrupole moments.^{1,2,22} The sign of $\chi(2_2^+)$ is related to the sign of P_4 defined as $P_4 \equiv M_{E2}(0^+, 2_1^+) M_{E2}(2_1^+, 2_1^+) M_{E2}(0^+, 2_2^+) M_{E2}(2_1^+, 2_2^+)$, which has been determined to be negative.³⁰ (Our definition of the reduced matrix elements includes an i^λ phase factor.) Since muonic experiments have established the sign of $M_{E2}(2_1^+, 2_1^+)$ to be positive,³¹ the sign of $\chi(2_2^+)$ is determined unambiguously. The magnitude of $\chi(2_2^+)$ was taken from the previous measurements,^{1,2,23,24} and was modified to agree with the 2_2^+ branching ratios determined in this experiment.

IV. EXPERIMENTAL RESULTS

The extracted $q(2_2^+)$ values for Os isotopes, along with those of ^{184,186}W (Ref. 18) and ¹⁹⁴Pt (Ref. 17) are shown in Table I. A short description of how the values were obtained will be given in the following subsections. Also included in this table are the predictions of (i) microscopic models, namely the pairing-plus-quadrupole (PPQ) model of Kumar and Baranger,⁴ and boson expansion theory (BET) of Weeks, Kishimoto, and Tamura,⁸ (ii) phenomenological models, including the dynamic collective model (DCM) of Sedlmayr *et al.*,^{10,34} interacting boson approximation (IBA),¹⁴

and asymmetric rotor model with variable moment of inertia (ARM+VMI) due to Toki and Faessler.³³ To make a meaningful comparison between these models, the results of PPQ, BET, and DCM calculations were scaled by matching the calculated $M_{E2}(0^+ \rightarrow 2_1^+)$ values to the adopted experimental results shown in Tables I and II.

The experimental $q(2_1^+)$ values of ^{190,192}Os relative to that of ¹⁸⁸Os were obtained through a procedure which is quite analogous to that described in Sec. III. Due to smaller excitation energy, the reorientation effect is smaller for the 2_1^+ states compared to the 2_2^+ states. As a result, the uncertainties in the deduced relative quadrupole moments are rather large. Nevertheless, such information serves as an additional check on the reliability of the method and the extracted quantities. The values obtained in the experiment are shown in Table II. Table III compares the branching ratios $B_R(2_2^+)$ obtained in this survey with other measurements and the theoretical predictions of the above models.

A. ¹⁸⁸Os nucleus

The spectroscopic quadrupole moments of the 2_1^+ and 2_2^+ states were deduced from the particle spectroscopy data to be $q(2_1^+) = -1.15(25)$ e b, and $q(2_2^+) = +1.05(30)$ e b. The extracted value for

TABLE I. Comparison of the experimental and theoretical values for the spectroscopic quadrupole moments of the 2_2^+ states. Theoretical predictions are scaled to reproduce the adopted experimental $M(E2; 0^+ \rightarrow 2_1^+)$ transition moments shown in the table. Values are given in units of (e b).

	Experimental values ^a			Adopted $M(E2; 0^+ \rightarrow 2)$	Theoretical predictions					
	Particle	Particle- γ	Average		PPQ ^b	BET ^c	IBA1 ^d	IBA2 ^e	DCM ^f	ARM ^g
¹⁸⁴ W		0.1(4) ^h		-1.94 ^h	0.74			1.62	1.55	1.7
¹⁸⁶ W	1.5(4)	1.1(3)	1.3(3) ^h	-1.83 ^h	1.03			1.54	1.64	1.6
¹⁸⁸ Os	1.05(30)	0.83(45)	1.00(25)	-1.68 ⁱ	1.14	1.42	1.39	1.21	1.46 ^j	1.38
¹⁹⁰ Os		0.9(4)		-1.55 ⁱ	0.85	1.27	1.23	1.20	1.34 ^j	1.17
¹⁹² Os		0.8(3)		-1.44 ⁱ	0.33	1.01	1.0	0.97	1.02 ^j	0.81
¹⁹² Pt				1.37 ^k	-0.49	-0.32	+0.02	+0.22	-0.54	-0.86
¹⁹⁴ Pt		-0.50(45) ^l		1.27 ^l	-0.41	-0.49	+0.01	-0.15	-0.65	-0.21
¹⁹⁶ Pt				1.23 ^m	-0.62	-0.55	0.0	-0.18	-0.54	0.0

^a Values in parentheses represent uncertainties in the least significant digits.

^b Pairing-plus-quadrupole model, Ref. 4.

^c Boson expansion theory, Ref. 8.

^d Interacting boson approximation (one boson), Ref. 14.

^e Interacting boson approximation (two bosons), Ref. 32.

^f Dynamics collective model, Ref. 10.

^g Asymmetric rotor model plus variable moment of inertia, Ref. 33. The asymmetry parameters γ are taken to be 13.7°, 16.0°, 19.1°, 21.7°, 25.2°, 24.4°, 28.8°, and 30° for ^{184,186}W, ^{188,190,192}Os, and ^{192,194,196}Pt, respectively.

^h Reference 18.

ⁱ Average of reported values in Refs. 1, 2, 23 and 24.

^j Reference 34.

^k Reference 35.

^l Reference 17.

^m Average of values reported in Refs. 3 and 24.

TABLE II. Comparison of experimental and theoretical values for the spectroscopic quadrupole moments of the 2_1^+ states. Theoretical predictions are scaled to reproduce the adopted experimental $M(E2;0^+ \rightarrow 2_1^+)$ transition moments shown in the table. Values are given in units of ($e b$).

	Experimental values ^a			Theoretical predictions ^c						
	Present work	Previous Coul ex.	Muonic	Adopted ^b $M(E2;0 \rightarrow 2)$	PPQ	BET	IBA1	IBA2	DCM	ARM
¹⁸⁴ W		-1.65(17) ^d		-1.94	-1.7			-1.75	-1.7	-1.7
¹⁸⁶ W		-1.35(17) ^d		-1.83	-1.51			-1.65	-1.6	-1.6
¹⁸⁸ Os	-1.15(25) ^e	-1.33(9) ^f	-1.47(4) ^g	-1.68	-1.18	-1.46	-1.42	-1.27	-1.4	-1.38
¹⁹⁰ Os	-0.8(3) ^h	-0.98(8) ^f		-1.55	-0.86	-1.28	-1.23	-1.21	-1.3	-1.17
	-0.95(30) ⁱ		-1.18(3) ^g							
¹⁹² Os	-0.7(3) ^h	-0.53(10) ^f		-1.44	-0.32	-1.0	-1.0	-0.98	-1.0	-0.81
	-0.8(3) ⁱ		-0.97(3) ^g							
¹⁹² Pt		+0.62(6) ^f		1.37	+0.09	+0.35	-0.025	-0.136	+0.46	+0.86
¹⁹⁴ Pt		+0.63(6) ^f	0.25(17) ^j	1.27	+0.48	+0.53	-0.013	+0.123	+0.58	+0.21
¹⁹⁶ Pt		+0.78(6) ^f		1.23	+0.74	+0.63	0.0	+0.29	+0.48	0.0

^a Values in parentheses represent uncertainties in the least significant digits.

^b References are given in Table I.

^c Description and references are given in Table I.

^d Reference 36.

^e Particle spectroscopy data.

^f Average of reorientation measurements by the Pittsburgh group (Refs. 1-3) and Rochester group (Ref. 22).

^g Reference 31.

^h From particle- γ coinc. data assuming $q(2_1^+) = -1.33 e b$ for ¹⁸⁸Os from reorientation measurements.

ⁱ From particle- γ coinc. data assuming $q(2_1^+) = -1.47 e b$ for ¹⁸⁸Os from muonic experiments.

^j Reference 37.

$q(2_1^+)$ is in reasonable agreement with $\langle q(2_1^+) \rangle = -1.33(9) e b$, which is the average of the previous reorientation measurements.^{1,2,22}

The result of particle- γ coincidence data may be expressed as

$$q(2_2^+) = 0.83(45) + 0.30[q(2_1^+) - (-1.3)] - 0.08[\chi(2_2^+) - (-3.13)] e b, \quad (6)$$

where the values $q_0(2_1^+) = -1.3 e b$ and $\chi_0(2_2^+) = -3.13 e b$ were used in the calculation. Variations in $q(2_2^+)$ due to changes in $q(2_1^+)$ and $\chi(2_2^+)$ are readily calculable from this equation. This result is in reasonable accord with that obtained in the particle spectroscopy experiment. Considering the fact that the two methods are quite different, the close agreement between the two independent

TABLE III. Comparison of the experimental and theoretical branching ratios $B(E2;2_2^+ \rightarrow 2_1^+)/B(E2;2_2^+ \rightarrow 0^+)$.

	Experimental values ^a			Theoretical values ^b				
	Pittsburgh	Other measurements	PPQ	BET	IBA1	IBA2	DCM	ARM
¹⁸⁴ W	2.1(1) ^c	1.80(5) ^d	10.3			1.9	7.9	2.4
¹⁸⁶ W	2.3(1) ^c	2.2(1) ^d	9.8			2.1	5.7	3.0
¹⁸⁸ Os	3.5(2) ^e	3.2(4) ^d	10.9	2.6	3.0	2.9	18.9	4.6
¹⁹⁰ Os	5.4(2) ^e	5.7(8) ^d	18.8	3.1	4.4	5.5	127	7.5
¹⁹² Os	7.6(4) ^e	8.4(4) ^d	106	5.6	7.4	9.7	∞	22.1
¹⁹² Pt		200 ^g	555	312	25 000	492	∞	26.4
¹⁹⁴ Pt	261(10) ^h	290(30) ⁱ	451	50 000	50 000	16 300	∞	361
¹⁹⁶ Pt		140 000 ^j	70	526	100 000	410	1975	∞

^a Values in parentheses represent uncertainties in the least significant digits.

^b Description and references given in Table I.

^c Reference 18.

^d Reference 24.

^e Present work.

^f Reference 25.

^g Reference 38.

^h Reference 17.

ⁱ Average of values listed in Ref. 17.

^j Reference 14.

measurements is reassuring. The adopted value of $q(2_2^+) = 1.0 \pm 0.25$ e b is based on the weighted average of the results of the two experiments.

B. ^{190}Os nucleus

The value for $q(2_2^+)$, extracted from the slope of the sensitivity plot, was found to be

$$q(2_2^+) = 0.5(3) + 0.36[q(2_1^+) - (-0.98)] - 0.26[\chi(2_2^+) - (-3.61)] \text{ e b.} \quad (7)$$

This result is based on a least-squares fit to all six experimental points. It is worth noting that the $(2_2^+ \rightarrow 0^+)$ yield from the α beam was inexplicably large. Omitting this point from the fit, one obtains a value of $0.85(40)$ e b for the true slope.

As mentioned earlier, the $(2_1^+ \rightarrow 0^+)$ transition γ rays may be utilized to extract the relative spectroscopic quadrupole moments of the 2_1^+ states. The analysis of the data resulted in the relationship

$$[q(2_1^+)]^{190} - 0.904[q(2_1^+)]^{188} = 0.4(3) \text{ e b.} \quad (8)$$

For an adopted value of $[q(2_1^+)]^{188} = -1.3$ e b, the above equation renders $[q(2_1^+)]^{190} = -0.8(3)$ e b.

Again, it is worth recalling that according to Eq. (5) of Sec. III, the extracted $q(2_2^+)$ depends on the experimental $q(2_1^+)$ value. Therefore, for a more realistic estimate of $q(2_2^+)$, it is desirable to use $[q(2_1^+)]^{\text{exp}} = -0.8$ e b in Eq. (7). This results in $q(2_2^+) = 0.55(30)$, or $0.9(4)$ e b for the ^{190}Os nucleus, depending on whether the $(2_2^+ \rightarrow 0^+)$ γ -ray yield due to the α beam is included in the fit or not.

C. ^{192}Os nucleus

The static quadrupole moment of the 2_2^+ state was determined from the sensitivity plot of Fig. 5 to be

$$q(2_2^+) = 0.9(3) + 0.42[q(2_1^+) - (-0.5)] - 0.29[\chi(2_2^+) - (-3.87)] \text{ e b.} \quad (9)$$

The relative $q(2_1^+)$ values of ^{188}Os and ^{192}Os may be expressed as

$$[q(2_1^+)]^{192} - 0.846[q(2_1^+)]^{188} = 0.4(3) \text{ e b.} \quad (10)$$

This relationship gives $[q(2_1^+)]^{192} = -0.7(3)$ e b if one assumes a value of -1.3 e b for the $q(2_1^+)$ in the ^{188}Os nucleus. This may be compared with $[q(2_1^+)]^{192} = -0.53(10)$ e b, which is the average of previous reorientation measurements.

As discussed in the previous subsection, a more realistic estimate of $q(2_2^+)$ is obtained if one substitutes $[q(2_1^+)]^{\text{exp}} = -0.7$ e b in Eq. (9). The resulting value for $q(2_2^+)$ is then $0.8(3)$ e b. Similarly,

if $q(2_1^+) = -1.0$ of the muonic experiment were substituted in Eq. (9), the deduced $q(2_2^+)$ would be further reduced to $0.7(3)$ e b.

V. DISCUSSION

Many features in the energy spectra of the heavy transitional nuclei suggest the rapid onset of triaxiality and prolate to oblate shape transition in this region. According to Kumar,³⁹ the prolate-oblate difference in the potential energy V_{p_0} and the static quadrupole moment of the 2_1^+ state are strongly correlated with the $(E_{2_2^+} - E_{4_1^+})$ energy difference. The near degeneracy of the 2_2^+ and 4_1^+ states in the heavier Os isotopes and subsequent drop of the 2_2^+ state below 4_1^+ would imply a prolate-oblate shape transition in the $A \approx 190$ mass region, where the $E_{2_2^+}/E_{2_1^+}$ energy ratio attains a minimum.

Experimentally, the first clear evidence in support of the above expectations was offered by Saladin and co-workers, who measured the spectroscopic quadrupole moment of the 2_1^+ states, $q(2_1^+)$, in Os (Refs. 1, 2) and Pt (Ref. 3) nuclei. The reduction in magnitude of the $q(2_1^+)$ values compared to the rigid rotor values (by as much as 50% for $A \approx 190$ nuclei), and the change in sign confirmed the earlier predictions of Kumar and Baranger.⁴

Since then, a wealth of experimental data has been accumulated and interpreted within the framework of one or another of the many triaxial models. While all these models agree on the presence of significant triaxiality in this region, they differ on the question of its origin and nature. The more microscopic calculations such as pairing-plus-quadrupole (PPQ) of Kumar and Baranger,⁴ microscopic calculation of potential energy surfaces by Mosel and Greiner,⁵ boson expansion theory (BET) of Weeks, Kishimoto, and Tamura,^{7,8} as well as a Hartree-Fock-Bogoliubov calculation by Girod and Grammaticos¹¹ predict a significant softness with respect to γ vibrations in this region. Similar conclusions have been reached in a semi-microscopic calculation by Gotz *et al.*⁶ and in some phenomenological models, including the collective dynamical model (CDM) of Sedlmayr *et al.*^{10,34} and the IBA of Iachello and Arima.¹³

In contrast to the above models, the ARM of Davydov and Filippov¹² assumes a core which is rigid with respect to γ vibrations. This model has been extended to include the following: (i) γ vibrations⁴⁰ or both γ and β vibrations⁴¹ to account for the excited 0^+ and 2^+ states; (ii) variable moment of inertia (ARM + VMI), or the 0 and 2 quasi-particle coupling in order to lower the energies of the high spin states³³ and correct for the phase of

odd-even clustering in the quasigamma band⁴²; (iii) coupling of an odd nucleon in a single,⁴³ or several^{44,45} Nilsson orbitals to explain the negative-^{43,44} and some positive-parity bands⁴⁵ in the transitional odd-*A* nuclei.

In the following subsections we shall briefly compare the experimental data with the predictions of the above models. The experimental information may be, broadly speaking, classified into the following categories.

(i) *Energies of the ground state and quasigamma band in the transitional even-even nuclei.* The microscopic pairing-plus-quadrupole⁴ and boson expansion theory^{7,8} models, and to a lesser extent the interacting boson approximation phenomenological model, give reasonable estimates of the energy levels of the ground-state band. The excitation energies of the ground-state band are, however, overestimated in a simple asymmetric rotor model.¹² This problem may be remedied by inclusion of a variable moment of inertia.³³ The phenomenological dynamic collective model^{10,34} fits both the ground-state band and gamma-band excitation energies very nicely. The difference between the γ -soft and γ -rigid potentials manifests itself in the odd-even staggering of the gamma-band energies: The energy levels of the gamma band in a γ -soft potential show a $(3^+, 4^+), (5^+, 6^+), \dots$ clustering pattern, which is opposite to the $(4^+, 5^+), (6^+, 7^+), \dots$ bunching pattern predicted by the rigid asymmetric rotor model. Although the experimental data show a slight $(3^+, 4^+), (5^+, 6^+), \dots$ clustering pattern, the observed odd-even staggering is noticeably smaller than that predicted by the above γ -soft models. Recently, Yadav *et al.*⁴² have shown that inclusion of 0 and 2 quasiparticle coupling in the asymmetric rotor model has the effect of both lowering the energies of the high spin states, and correcting the phase of odd-even staggering.

(ii) *Energies of the positive and negative parity bands in the transitional odd-*A* nuclei.* The negative parity bands in these nuclei were initially explained in terms of a particle-rigid asymmetric rotor model.⁴³ Inasmuch as the deduced core asymmetry agreed with the asymmetry of the neighboring even-even nuclei, the success of this model was interpreted as evidence in support of rigid triaxiality in this region. However, as Paar *et al.*⁴⁶ have shown, soft cores or even models within spherical representation have equal success in fitting not only the negative parity but also the positive parity bands in these nuclei. It is now believed that the odd particle is not a sensitive enough probe to distinguish between the quadrupole fields of various cores.^{47,48} In addition to quadrupole deformation and asymmetric

shapes, the presence of hexadecapole deformations in this region^{27,49} entails perturbation of the Nilsson states,⁵⁰ and would necessitate inclusion of several orbitals in any realistic calculation of energies in these odd-*A* nuclei.

(iii) *Energies and branching ratios of the excited 0^+ and 2^+ states.* In a series of (n, γ) experiments Casten and co-workers^{14,51} have established many excited 0^+ and 2^+ states below the pairing gap in Os and Pt nuclei. The recurring $0^+ - 2^+ - 2^+$ pattern of these states and their branching ratios are nicely explained by both the perturbed-O(6) limit of the IBA¹⁴ and the boson expansion theory.⁸ It should be noted that excited 0^+ states are forbidden in a simple rigid asymmetric model, which in addition, does not allow for any excited 2^+ state above the 2_2^+ level. The inclusion of β vibrations in this model will provide a β band and its associated 0^+ and 2^+ states.⁴⁰ Additional excited 2^+ states would require the inclusion of γ vibrations.⁴¹

(iv) *One and two nucleon transfer data.* Due to the shape difference between the initial and final nuclei, the two-neutron transfer cross section attains a local minimum in the shape transition region.⁵² Results of a ¹⁹²Os(¹²C, ¹⁴C)¹⁹⁰Os transfer experiment have shown only a weak direct $J=2$ pickup strength between ^{192,190}Os nuclei.⁵³ More recently, relative Pt(t, p) and Pt(p, t) ground state transfer strengths have been measured and interpreted within the framework of the limiting symmetries of the IBA.⁵⁴ The (t, p) data favor the O(6) or SU(3) limiting symmetries over the SU(5). Similarly, the O(6) limit of the IBA provides a qualitative explanation of $L=0$ and $L=2$ strengths in Pt(p, t) reactions. In contrast, the results of (d, p) and (d, t) reactions on even-even Os and Pt targets have not been conclusive. While the results rule out an interpretation of the low-lying states as members of a single asymmetric rotational band (such as those calculated by Hecht and Satchler⁵⁵), they cannot completely reject an explanation in terms of states obtained by admixing several asymmetric rotational bands.^{56,57} A better fit to the data was obtained in two model calculations. The first one is a Faessler-Greiner type⁹ which allows for the β and γ vibrations in the core. The second is a Nilsson calculation.⁵⁸ The predicted spectroscopic factors deviated from the experimental values for some low-lying states. Inclusion of hexadecapole deformation in these calculations, which perturbs the Nilsson model states and fragments the single particle strengths through Coriolis mixing,⁵⁰ may bring the model predictions closer to the experimental results.

(v) *Electromagnetic moments.* With the possible exception of the third category, the above experi-

mental information has not offered a unique and sensitive probe of the core softness. In contrast, the static and transition electromagnetic moments of the gamma band show a particular sensitivity to the asymmetry of the core and the extent of its softness with respect to γ vibrations.^{16,17} Specifically, the $B(E2; I_\gamma \rightarrow I_g)$ of the γ -band-ground band transitions changes $\sim 1/I$ in the γ -soft model of Jean-Wilets,¹⁵ but $\sim 1/I^2$ in the rigid asymmetric rotor model.¹⁶ Several groups have used heavy ions to Coulomb excite some Pt isotopes.^{38,59,60} While the results of the ^{136}Xe beam are compatible with a rigid triaxial interpretation of $^{192,194}\text{Pt}$ nuclei,⁵⁹ the $B(E2)$ values of the gamma band in ^{192}Pt obtained from the ^{84}Kr experiment³⁸ are larger than those of the ARM by a factor of 2. This may signify some softness in this core. Such discrepancies may be due to the fact that heavy ion Coulomb excitation of the higher lying members of the gamma band in these nuclei proceeds through several competing paths, each of which depends on many matrix elements. The data analysis is, therefore, complicated and involves some model assumptions which may inadvertently bias the results.¹⁷ To deduce model-independent matrix elements, one would have to start with lighter ions and gradually proceed to heavier beams, determining a few matrix elements at a time. Some efforts in this direction are currently underway.⁶¹ While the quadrupole moments of the 2_1^+ and 2_2^+ states are more sensitive to the average asymmetry $\langle \gamma \rangle$, rather than to its fluctuation $\sigma(\gamma)$, nevertheless, they enter the determination of the $B(E2)$ values of the gamma band rather sensitively. Similarly, quadrupole moment values are needed for the determination of the core softness $\sigma(\gamma)$ from nearly model independent sum rules given by Kumar.⁵² In the following, we shall compare the experimental values of $q(2_1^+)$, $q(2_2^+)$, and the branching ratios of the (2_2^+) states with predictions of several microscopic and phenomenological models.

A. Systematics of $q(2_1^+)$ in W-Os-Pt region

A graphical representation of Table II, which compares the experimental and theoretical values of $q(2_1^+)$, is given in Fig. 6. The Coulomb excitation measurements (full circles) for Os and Pt nuclei are a weighted average of the values reported by the Pittsburgh¹⁻³ and Rochester²² groups. The corresponding values for $^{184,186}\text{W}$ are from recent experiments at Rochester.³⁶ Also shown in this figure are the muonic measurements³¹ (full squares).

It is noteworthy that the results of the muonic measurements³¹ differ increasingly from the re-

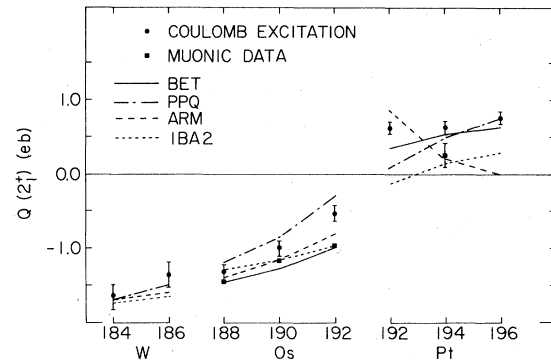


FIG. 6. Comparison of the experimental spectroscopic quadrupole moments of the 2_1^+ states with predictions of various models. The full circles represent the weighted average of the reorientation measurements, and full squares are from muonic experiments (Ref. 31) (see Table II). The labels BET, PPQ, ARM, and IBA2 refer to boson expansion theory (Ref. 8), pairing-plus-quadrupole (Ref. 4), asymmetric rotor model (Ref. 33), and 2 boson interacting boson approximation (Ref. 32), respectively.

orientation values, as one moves toward heavier nuclei. The difference is particularly large for ^{192}Os and ^{194}Pt nuclei. A similar difference has been observed in the Hg region, where the muonic experiments (a) underestimate the quadrupole moment of ^{198}Hg (Ref. 62) relative to a reorientation experiment, and (b) obtain the opposite sign for the quadrupole moment of the $(\frac{3}{2}^-)$ state in ^{199}Hg (Ref. 62) compared to a Mossbauer experiment.⁶³ Interestingly, in all these cases the quadrupole moments deduced in muonic experiments fall systematically below the values obtained in the reorientation measurements; i.e., they tend toward more prolate shapes. In contrast, the results of the muonic experiments are in excellent accord with Coulomb excitation measurements for such nuclei as ^{152}Sm (Ref. 64) and ^{175}Lu ,⁶⁵ which are generally believed to have symmetric charge distributions. Therefore, the systematic discrepancy between the muonic and Coulomb excitation measurements in the heavy transitional region may prove to be significant. At present, one could only speculate about factors responsible for such a systematic difference. One possible reason cited in the literature,⁶⁶ namely the influence of giant dipole resonance (GDR) on the extraction of quadrupole moments in the reorientation experiments, does not seem to be a viable explanation. While some of these measurements are only weakly sensitive to the GDR effects, others² are based on relative measurement of the quadrupole moment, and hence are independent of the polarization effect. In contrast to the Coulomb excitation mea-

surements which are model independent [in the sense that no specific charge distribution enters the extraction of $q(2^+)$], the results of the muonic experiments depend on the assumptions made for the nuclear charge distribution. The analysis of the muonic experiments have so far included only axially symmetric charge distributions.⁶⁷ However, since axial asymmetry plays a very important role in this transitional region, and in view of the fact that the above differences seem to be correlated with the asymmetry parameter, it will be interesting to explore the influence of an asymmetric charge distribution on the analysis of muonic data. One such study has already demonstrated a significant sensitivity to asymmetric charge distributions in the case of $3D-2P$ muonic transition energies.⁶⁸

Considering all $q(2_1^+)$ values, the predictions of PPQ and BET are in better agreement with the systematic trend than ARM and IBA. The asymmetry parameters used for the ARM calculations are those given by Toki and Faessler (ARM+VMI).³³ While the predictions of the absolute values of quadrupole moments in the ARM (quadrupole signs are not predicted in this model) are in close agreement with the experimental measurements for W and Os, they follow the wrong trend in Pt isotopes.

The quadrupole moments of the 2_1^+ and 2_2^+ states vanish in the O(6) limit of the one boson interacting boson approximation (IBA1). Therefore, as shown in Table II, perturbed O(6) calculations,¹⁴ which describe the Pt-Os region in terms of an O(6) \rightarrow rotor transition, predict very small (prolate) quadrupole moments for Pt nuclei. (The seemingly more rotational bands in Os and lighter Pt nuclei are reproduced by the introduction of a $Q \cdot Q$ interaction in these calculations.) The calculated values, however, are in good accord with the muonic measurements for Os isotopes. Inclusion of two bosons (proton and neutron bosons) in this model, IBA2, results in a slightly improved prediction for the Pt isotopes and leaves the Os values essentially unchanged.³² The sign of the spectroscopic quadrupole moment is still predicted to be negative (prolate) for ¹⁹²Pt, in contradiction with the experiment.

B. Systematics of $q(2_2^+)$ in W-Os-Pt region

The experimental $q(2_2^+)$ values, along with some model predictions, are given in Table I and presented in Fig. 7. The quadrupole moment of the 2^+ member of the quasigamma band is predicted to be $\approx -q(2_1^+)$ in almost all models. Within the experimental uncertainties, this relationship seems to be valid for ¹⁸⁶W, ^{188,190,192}Os, and ¹⁹⁴Pt nuclei. In contrast, $q(2_2^+)$ is measured to be much

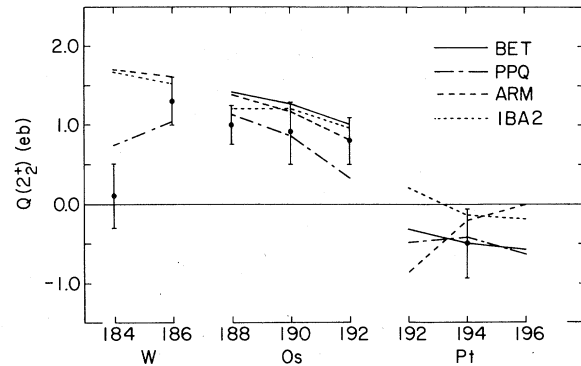


FIG. 7. Comparison of the experimental spectroscopic quadrupole moments of the 2_2^+ states (full circles) with various model predictions. The labels are the same as in Fig. 6.

smaller than $q(2_1^+)$ for ¹⁸⁴W. The pairing-plus-quadrupole and, to a lesser extent, dynamical collective models are the only models which predict a drop in $q(2_2^+)$ from ¹⁸⁶W to ¹⁸⁴W. (The predictions of the boson expansion theory are not presently available for W isotopes.) Within the framework of PPQ, this decrease is caused by admixture of some $K=0$ (β -band) component in the wave function of the 2_2^+ state in ^{182,184}W. Since $q(2_2^+) \approx -q(2_1^+)$, the predicted admixture of $K=0$ and $K=2$ components (that is, coupling of β and γ degrees of freedom) would result in reduced quadrupole moments for the 2_2^+ state in these nuclei. A preliminary measurement of $q(2_2^+)$ in ¹⁸²W has confirmed the above predicted reduction.⁶⁹

For the Os isotopes, all models are in reasonable agreement with the data. With increasing neutron number, the PPQ predicts a faster drop in $q(2_2^+)$ than the experimental trend.

In the Pt region, lack of experimental systematics prevents a close scrutiny of the model predictions. However, should the observed trend of $q(2_2^+) \approx -q(2_1^+)$ continue, the above mentioned (subsection V A) shortcomings of ARM and IBA would persist for the 2_2^+ state as well.

C. Systematics of the branching ratio of the 2_2^+ state

Table III compares the experimental branching ratios $B_R(2_2^+) \equiv B(E2; 2_2^+ \rightarrow 2_1^+)/B(E2; 2_2^+ \rightarrow 0_1^+)$ with some model predictions. Starting with ¹⁸⁴W, the experimental branching ratios gradually increase with increasing proton and neutron number, until they reach a maximum in ¹⁹⁶Pt (Fig. 8). Although nearly all models reproduce the general experimental trend, ARM gives the best quantitative agreement. All γ -soft models (both microscopic

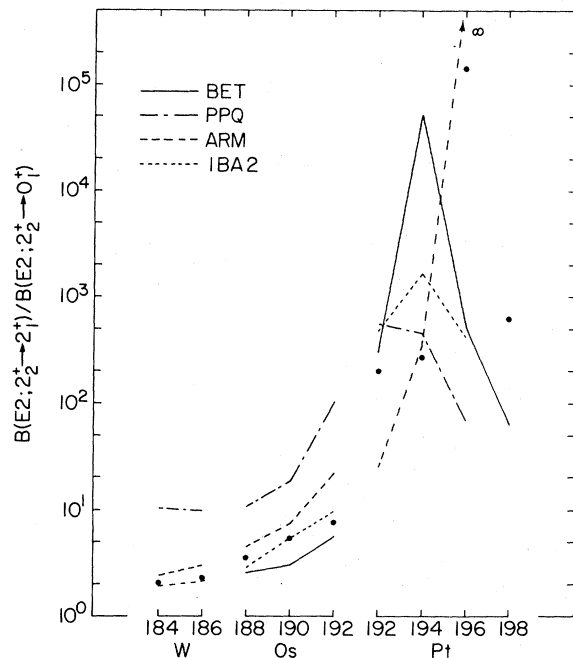


FIG. 8. Comparison of the experimental (full circles) and theoretical branching ratios of the 2_2^+ states. The labels are the same as in Fig. 6.

and phenomenological) predict a maximum peak at ^{194}Pt rather than ^{196}Pt .

It has been pointed out that ARM fails to reproduce the experimental quadrupole moments and $B_R(2_2^+)$ simultaneously.¹⁷ This shortcoming is similarly shared by IBA1, which fails to reduce $B(E2; 2_2^+ \rightarrow 0_1^+)$ values without concurrently reducing the quadrupole moments. Figure 9 shows a plot of $q(2_1^+)/M_{E2}(0^+, 2_2^+)$. Although the experimental values change by nearly two orders of magnitude, the predictions of ARM (and IBA1) remain nearly constant across the W-Os-Pt nuclei, where the asymmetry parameter changes from $\approx 14^\circ$ in ^{184}W to $\approx 30^\circ$ in ^{196}Pt . In contrast, the general trend is reproduced by the PPQ and BET microscopic models, as well as the more realistic version of IBA, namely IBA2.

VI. SUMMARY

Spectroscopic quadrupole moments of the 2_1^+ and 2_2^+ states, as well as branching ratios $B_R(2_2^+)$ in $^{188, 190, 192}\text{Os}$ isotopes have been measured. The results, together with the corresponding values for the neighboring W and Pt nuclei are compared with several microscopic and phenomenological models. The general experimental trends are best reproduced by the microscopic pairing-plus-quadrupole and boson expansion theories. In

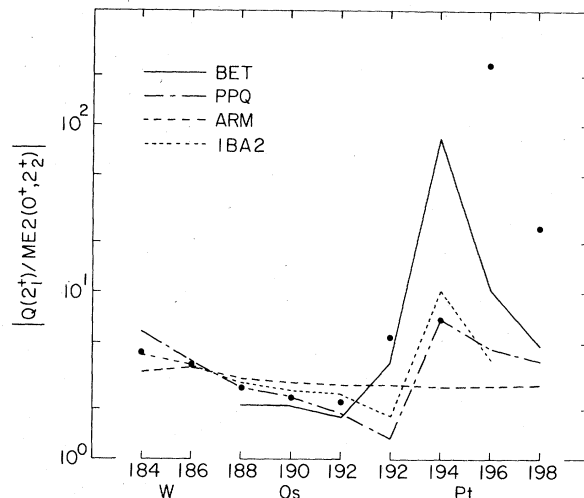


FIG. 9. Comparison of the experimental (full circles) and theoretical values of $q(2_1^+)/M_{E2}(0^+, 2_2^+)$ ratios. The labels are the same as in Fig. 6.

particular, the success of PPQ in reproducing both the fall in $q(2_2^+)$ in the lighter W isotopes and nonvanishing quadrupole moments in the Pt region is very impressive. The predictions of the phenomenological dynamical collective model are in reasonable accord with the experimental data. Both (one boson) interacting boson approximation and asymmetric rotor models have difficulty fitting the quadrupole moments in the Pt nuclei. The more realistic two boson IBA, which includes both proton and neutron bosons, gives somewhat improved results. The gross macroscopic properties of the nuclei in this transitional region, therefore, seem to be quite responsive to subtle changes in the underlying microscopic structure.⁵ The present results, along with other experimental evidence briefly reviewed in this paper, indicate that compared to the rigid triaxial models the γ -soft models have had better or equal success in explaining the systematics of these transitional nuclei.

ACKNOWLEDGMENTS

The authors wish to thank Dr. R. F. Casten for many useful discussions and his assistance in performing the IBA1 calculations. We are also indebted to Dr. D. Cline, Dr. K. T. Weeks, and Dr. A. E. L. Dieperink for communication of their results prior to publication. This work was supported in part by a grant from the National Science Foundation (University of Pittsburgh) and in part by the Division of Basic Energy Sciences, U. S. Department of Energy, under Contract No. DE-AC02-76CH00016 (BNL).

- *Present address.
 †Present address: Gulf Research and Development Co., P.O. Drawer 2038, Pittsburgh, Pennsylvania 15230.
 ‡Present address: Brookhaven National Laboratory, Upton, New York 11973.
- ¹R. J. Pryor and J. X. Saladin, *Phys. Rev. C* **1**, 1573 (1970).
 - ²S. A. Lane and J. X. Saladin, *Phys. Rev. C* **6**, 613 (1972).
 - ³J. E. Glenn and J. X. Saladin, *Phys. Rev. Lett.* **20**, 1298 (1968).
 - ⁴K. Kumar and M. Baranger, *Nucl. Phys.* **A122**, 273 (1968).
 - ⁵U. Mosel and W. Greiner, *Z. Phys. A* **217**, 256 (1968).
 - ⁶U. Gotz, H. C. Pauli, and K. Alder, *Nucl. Phys.* **A192**, 1 (1972).
 - ⁷T. Kishimoto and T. Tamura, *Nucl. Phys.* **A270**, 317 (1976).
 - ⁸K. J. Weeks and T. Tamura, *Phys. Rev. Lett.* **44**, 533 (1980); K. J. Weeks, private communication.
 - ⁹A. Faessler and W. Greiner, *Z. Phys.* **168**, 425 (1962); **170**, 105 (1962); **177**, 190 (1964); A. Faessler, W. Greiner, and R. K. Sheline, *Nucl. Phys.* **70**, 33 (1965).
 - ¹⁰R. Sedlmayr, M. Sedlmayr, and W. Greiner, *Nucl. Phys.* **A232**, 465 (1974); M. Sedlmayr, Ph.D. thesis, University of Frankfurt (unpublished); W. Greiner, private communications.
 - ¹¹M. Girod and B. Grammaticos, *Phys. Rev. Lett.* **40**, 361 (1978).
 - ¹²A. S. Davydov and G. Filippov, *Nucl. Phys.* **8**, 237 (1958).
 - ¹³A. Arima and F. Iachello, *Phys. Rev. Lett.* **40**, 385 (1978); A. Arima and F. Iachello, *Ann. Phys. (N.Y.)* **123**, 468 (1979).
 - ¹⁴R. F. Casten and J. A. Cizewski, *Nucl. Phys.* **A309**, 477 (1978).
 - ¹⁵L. Wilets and M. Jean, *Phys. Rev.* **102**, 788 (1956).
 - ¹⁶J. Meyer-ter-Vehn, *Phys. Lett.* **84B**, 10 (1979).
 - ¹⁷C. Baktash, J. X. Saladin, J. J. O'Brien, and J. G. Alessi, *Phys. Rev. C* **18**, 131 (1978).
 - ¹⁸J. J. O'Brien, J. X. Saladin, C. Baktash, and J. G. Alessi, *Nucl. Phys.* **A291**, 510 (1977).
 - ¹⁹J. X. Saladin, C. Baktash, J. J. O'Brien, and J. G. Alessi, in *Proceedings of the International Conference on Nuclear Structure, Tokyo, 1977* (International Academic Printing Co. Ltd., Tokyo, 1977), Vol. 1, p. 426.
 - ²⁰A. Winther and J. de Boer, in *Coulomb Excitation*, edited by K. Alder and A. Winther (Academic, New York, 1966), p. 303.
 - ²¹F. Roesel, J. X. Saladin, and K. Alder, *Comput. Phys. Commun.* **8**, 35 (1974).
 - ²²P. Russo, D. Cline, and J. Sprinkle, *Bull. Am. Phys. Soc.* **22**, 545 (1977); J. Sprinkle, D. Cline, and P. Russo, *ibid.* **22**, 545 (1977), and private communication.
 - ²³P. H. Stelson and L. Grodzins, *Nucl. Data Sect. A* **1**, 21 (1965).
 - ²⁴W. T. Milner, F. K. McGowan, R. L. Robinson, P. H. Stelson, and R. O. Sayer, *Nucl. Phys.* **A177**, 1 (1971).
 - ²⁵R. F. Casten, J. S. Greenberg, S. H. Sie, G. A. Burington, and D. A. Bromley, *Phys. Rev.* **187**, 1532 (1969).
 - ²⁶K. S. Krane, *At. Data Nucl. Data Tables* **16**, 383 (1975).
 - ²⁷F. T. Baker, T. H. Kruse, W. Hartwig, I. Y. Lee, and J. X. Saladin, *Nucl. Phys.* **A258**, 43 (1976).
 - ²⁸L. C. Northcliffe and R. F. Schilling, *Nucl. Data Tables* **A7**, 233 (1970).
 - ²⁹D. C. Camp and A. L. VanLehn, *Nucl. Instrum. Methods* **76**, 192 (1969).
 - ³⁰F. T. Baker, A. Scott, T. H. Kruse, W. Hartwig, E. Ventura, and W. Savin, *Phys. Rev. Lett.* **37**, 1931 (1976).
 - ³¹M. V. Hoehn, E. B. Shera, Y. Yamazaki, and R. M. Steffen, *Phys. Rev. Lett.* **39**, 1313 (1977).
 - ³²Values for W are from P. D. Duval and B. R. Bruce (unpublished); values for Os and Pt are from A. E. L. Dieperink, R. Bijker, and O. Scholten, private communication.
 - ³³H. Toki and A. Faessler, *Z. Phys. A* **276**, 35 (1976).
 - ³⁴R. Sedlmayr, M. Sedlmayr, and H. Stock, *Nucl. Phys.* **A303**, 393 (1978).
 - ³⁵R. M. Ronningen, R. B. Piercey, A. V. Ramayya, J. H. Hamilton, S. Raman, P. H. Stelson, and W. K. Dagenhart, *Phys. Rev. C* **16**, 571 (1977).
 - ³⁶P. Russo, J. K. Sprinkle, D. Cline, P. B. Vold, and R. P. Scharenberg, private communication.
 - ³⁷M. V. Hoehn, E. B. Shera, H. D. Wohlfahrt, Y. Yamazaki, R. M. Steffen, *Bull. Am. Phys. Soc.* **24**, 53 (1979).
 - ³⁸C. Roulet, H. Sergolle, P. P. Hubert, and T. Lindblad, *Phys. Scr.* **17**, 487 (1978).
 - ³⁹K. Kumar, *Phys. Rev. C* **1**, 369 (1970).
 - ⁴⁰A. S. Davydov and A. A. Shaban, *Nucl. Phys.* **20**, 499 (1960).
 - ⁴¹A. S. Davydov, *Nucl. Phys.* **24**, 682 (1961).
 - ⁴²H. L. Yadav, H. Toki, and A. Faessler, *Phys. Lett.* **76B**, 144 (1978).
 - ⁴³J. Meyer-ter-Vehn, *Nucl. Phys.* **A249**, 111 (1975); **A249**, 144 (1975).
 - ⁴⁴Ch. Vieu, S. E. Larsson, G. Leander, I. Ragnarsson, W. De Wieclawik, and J. S. Dionisio, *J. Phys. G* **4**, 1159 (1978).
 - ⁴⁵Ch. Vieu, S. E. Larsson, G. Leander, I. Ragnarsson, W. De Wieclawik, and J. S. Dionisio, *J. Phys. G* **4**, 531 (1978).
 - ⁴⁶V. Paar, Ch. Vieu, and J. S. Dionisio, *Nucl. Phys.* **A284**, 199 (1977).
 - ⁴⁷F. Donau and S. Faruendorf, *Phys. Lett.* **71B**, 263 (1977).
 - ⁴⁸P. Kemnitz, F. Donau, L. Funke, H. Strusny, D. Venos, and J. Meyer-ter-Vehn, *Nucl. Phys.* **A293**, 314 (1977).
 - ⁴⁹I. Y. Lee, J. X. Saladin, C. Baktash, J. E. Holden, and J. O'Brien, *Phys. Rev. Lett.* **33**, 383 (1974); F. T. Baker, A. Scott, T. H. Kruse, W. Hartwig, E. Ventura, and W. Savin, *Nucl. Phys.* **A266**, 345 (1976).
 - ⁵⁰R. F. Casten, D. D. Warner, and J. A. Cizewski, *Nucl. Phys.* **A333**, 237 (1980), and references therein.
 - ⁵¹J. A. Cizewski, R. F. Casten, G. J. Smith, M. R. Macphail, M. L. Stelts, W. R. Kane, H. G. Borner, and W. F. Davidson, *Nucl. Phys.* **A323**, 349 (1979); R. F. Casten, M. R. Macphail, W. R. Kane, D. Breitig, K. Schreckenbach, and J. A. Cizewski, *ibid.* **A316**, 61 (1979); R. F. Casten, H. G. Borner, J. A. Pinston, and W. F. Davidson, *ibid.* **A309**, 206 (1978).
 - ⁵²K. Kumar, in *The Electromagnetic Interaction in Nuclear Spectroscopy*, edited by W. D. Hamilton (North-Holland, Amsterdam, 1975), Chap. 3.
 - ⁵³D. L. Hanson, K. A. Erb, J. S. Vaagen, R. J. Ascutto,

- D. A. Bromley, and J. J. Kolata, Phys. Rev. C 16, 902 (1977).
- ⁵⁴P. T. Deason, C. H. King, T. L. Khoo, J. A. Nolen, and F. M. Bernthal, Phys. Rev. C 20, 927 (1979); J. A. Cizewski, E. R. Flynn, R. E. Brown, and J. W. Sunier, Phys. Lett. 88B, 207 (1979).
- ⁵⁵K. T. Hecht and G. R. Satchler, Nucl. Phys. 32, 286 (1962).
- ⁵⁶Y. Yamazaki and R. K. Sheline, Phys. Rev. C 14, 531 (1976).
- ⁵⁷D. Benson, P. Kleinheinz, R. K. Sheline, and E. B. Shera, Z. Phys. A 285, 405 (1978).
- ⁵⁸S. G. Nilsson, K. Dan. Vidensk. Selsk. Mat. Fys. Medd. 29, No. 16 (1955).
- ⁵⁹I. Y. Lee, D. Cline, P. A. Butler, R. M. Diamond, J. O. Newton, R. S. Simon, and F. S. Stephens, Phys. Rev. Lett. 39, 684 (1977).
- ⁶⁰K. Stelzer, F. Rauch, Th. W. Elze, Ch. E. Gould, J. Idzko, G. E. Mitchell, H. P. Nottrodt, R. Zoller, H. J. Wollersheim, and E. Emling, Phys. Lett. 70B, 297 (1977).
- ⁶¹C. Y. Wu, D. Cline, T. Czosnyka, L. Hasselgren, P. Russo, J. K. Sprinkle, I. Y. Lee, P. A. Butler, R. M. Diamond, F. S. Stephens, C. Baktash, and S. Steadman, Bull. Am. Phys. Soc. 25, 605 (1980).
- ⁶²A. A. Hahn, J. P. Miller, R. J. Powers, A. Zehnder, A. M. Rushton, R. E. Welsh, A. R. Kunselman, P. Roberson, and H. K. Walter, Nucl. Phys. A314, 361 (1979).
- ⁶³W. Wurtinger and E. Kankeleit, Z. Phys. A 293, 219 (1979).
- ⁶⁴Y. Yamazaki, E. B. Shera, M. V. Hoehn, and R. M. Steffen, Phys. Rev. C 18, 1474 (1978).
- ⁶⁵W. Dey, P. Ebersold, H. J. Leisi, F. Scheck, H. K. Walter, and A. Zehnder, Nucl. Phys. A326, 418 (1979).
- ⁶⁶W. Greiner, in *Nuclear Interactions*, edited by B. A. Robson (Springer, New York, 1979), p. 360.
- ⁶⁷L. K. Wagner, E. B. Shera, G. A. Rinker, and R. K. Sheline, Phys. Rev. C 16, 1549 (1977).
- ⁶⁸V. I. Bagaev, W. D. Fromm, I. N. Mikhailov, H. G. Ortlepp, V. Schmidt, and G. Musial, Phys. Lett. 67B, 169 (1977).
- ⁶⁹A. Hussein, J. X. Saladin, and C. Baktash, abstract contributed to the Proceedings of the International Conference on Nuclear Physics, Berkely, 1980, (LBL, to be published), Vol. 1, p. 111.